

Form Approved
OMB No. 0704-0188

PLEASE DO NOT RETURN YOUR FORM TO THE ABOVE ADDRESS.

[illegible]

1. REPORT DATE. Full publication date, including day, month, if available. Must cite at least the year and be Year 2000 compliant, e.g., 30-06-1998; xx-08-1998; xx-xx-1998.

2. REPORT TYPE. State the type of report, such as final, technical, interim, memorandum, master's thesis, progress, quarterly, research, special, group study, etc.

3. DATES COVERED. Indicate the time during which the work was performed and the report was written, e.g., Jun 1997 - Jun 1998; 1-10 Jun 1996; May - Nov 1998; Nov 1998.

4. TITLE. Enter title and subtitle with volume number and part number, if applicable. On classified documents, enter the title classification in parentheses.

5a. CONTRACT NUMBER. Enter all contract numbers as they appear in the report, e.g. F33615-86-C-5169.

5b. GRANT NUMBER. Enter all grant numbers as they appear in the report, e.g. 1F665702D1257.

5c. PROGRAM ELEMENT NUMBER. Enter all program element numbers as they appear in the report, e.g. AFOSR-82-1234.

5d. PROJECT NUMBER. Enter all project numbers as they appear in the report, e.g. 1F665702D1257; ILIR.

5e. TASK NUMBER. Enter all task numbers as they appear in the report, e.g. 05; RF0330201; T4112.

5f. WORK UNIT NUMBER. Enter all work unit numbers as they appear in the report, e.g. 001; AFAPL30480105.

6. AUTHOR(S). Enter name(s) of person(s) responsible for writing the report, performing the research, or credited with the content of the report. The form of entry is the last name, first name, middle initial, and additional qualifiers separated by commas, e.g. Smith, Richard, Jr.

7. PERFORMING ORGANIZATION NAME(S) AND ADDRESS(ES). Self-explanatory.

8. PERFORMING ORGANIZATION REPORT NUMBER. Enter all unique alphanumeric report numbers assigned by the performing organization, e.g. BRL-1234; AFWL-TR-85-4017-Vol-21-PT-2.

9. SPONSORING/MONITORING AGENCY NAME(S) AND ADDRESS(ES). Enter the name and address of the organization(s) financially responsible for and monitoring the work.

10. SPONSOR/MONITOR'S ACRONYM(S). Enter, if available, e.g. BRL, ARDEC, NADC.

11. SPONSOR/MONITOR'S REPORT NUMBER(S). Enter report number as assigned by the sponsoring/monitoring agency, if available, e.g. BRL-TR-829; -215.

12. DISTRIBUTION/AVAILABILITY STATEMENT. Use agency-mandated availability statements to indicate the public availability or distribution limitations of the report. If additional limitations/restrictions or special markings are indicated, follow agency authorization procedures, e.g. RD/FRD, PROPIN, ITAR, etc. Include copyright information.

13. SUPPLEMENTARY NOTES. Enter information not included elsewhere such as: prepared in cooperation with; translation of; report supersedes; old edition number, etc.

14. ABSTRACT. A brief (approximately 200 words) factual summary of the most significant information.

15. SUBJECT TERMS. Key words or phrases identifying major concepts in the report.

16. SECURITY CLASSIFICATION. Enter security classification in accordance with security classification regulations, e.g. U, C, S, etc. If this form contains classified information, stamp classification level on the top and bottom of this page.

17. LIMITATION OF ABSTRACT. This block must be completed to assign a distribution limitation to the abstract. Enter UU (Unclassified Unlimited) or SAR (Same as Report). An entry in this block is necessary if the abstract is to be limited.

Final Report

ONR Award No. N00014-99-1-0210

Neural Network Based Hyperspectral Algorithms

Principal Investigator: Grayson H. Rayborn

Associate Investigator: Ronald J. Holyer

University of Southern Mississippi

November 14, 2001

Work conducted under this grant has been reported at the following scientific conferences.

Ocean Optics XV
Muse'e Oceanographique, Monaco
October 16-20, 2000

International Conference "Current Problems in Optics of Natural Waters"
St. Petersburg, Russia
September 25-29, 2001

Printed proceedings from these conferences are attached and form the final technical report for this grant.

DISTRIBUTION STATEMENT A

Approved for Public Release
Distribution Unlimited

HYPERSENSPECTRAL BATHYMETRY ALGORITHMS FROM RADIATIVE TRANSFER MODELING

Ronald J. Holyer, David C. Hughes¹, Rachel P. Ingram

¹ *University of Southern Mississippi, School of Mathematical Sciences, Bldg. 9313, Rm 113, Stennis Space Center, MS, USA, 39529*

Juanita C. Sandidge

² *Naval Research Laboratory, Ocean Sciences Branch, Code 7334, Bldg. 1009, Rm. A114, Stennis Space Center, MS, USA, 39529-5004*

Walter F. Smith

³ *TASC, Bldg. 9313, Rm. 125, Stennis Space Center, MS, USA, 39529*

INTRODUCTION

In ocean optics the forward problem (*i.e.*, given water optical properties and illumination conditions, find the water-leaving radiance) is solved and several computer implementations of in-water radiative transfer are available. Using these radiative transfer models, water-leaving radiance can be calculated with precision limited only by the availability of computer resources. However, the inverse problem (*i.e.*, given observations of water-leaving radiance, find the water and illumination conditions that necessarily lead to this observation) is not solved in closed analytical form. The inverse relationship may even be many-to-one. Moreover solution of the inverse problem is the essence of remote sensing, where the objective is retrieval of water depth, water inherent optical properties, bottom reflectance, or some other parameter from observations of water-leaving spectral radiance or reflectance. In lieu of rigorous inversion, various empirical, semianalytical, statistical, or numerical methods have been utilized for retrieval of ocean parameters from remotely sensed spectral radiance data. We use a neural network to numerically model the inverse problem based on a synthetic data set produced by a radiative transfer model. This paper shows the result of that procedure applied to retrieval of water depth from hyperspectral imagery of the Ship Island area off the coast of Mississippi.

Sandidge and Holyer (1998) have applied a neural network to this problem previously. In the earlier work the neural network was trained using pixels in the hyperspectral image where depth is known from ground truth. Training directly from the image negates the need for atmospheric correction or normalization for illumination conditions and eliminates errors that may be caused by uncertainties in sensor calibration. Training directly from the image, however, does not result in universal relationships. A neural network trained using a Tampa Bay image, for example, would not be expected to produce good retrievals from the coastal waters of California. A more universal algorithm would be expected if the neural network were trained from a large data set including many water and bottom types and many illumination conditions. Cost and time required to obtain field observations leading to such an all-inclusive data set are prohibitive.

DISTRIBUTION STATEMENT A

Approved for Public Release
Distribution Unlimited

As an alternative to a large observational data set, we can take advantage of the fact that the forward problem has been solved and use a radiative transfer model to generate a diverse training set by numerical simulation. Lee *et al.*, (1998a) have used this approach with a semianalytical (SA) model to produce the synthetic training data. Their model included many approximations so that the remote sensing reflectance spectrum was completely defined by six parameters. Lee *et al.*, (1998a) reported the neural network trained to give an error of 18% on the training data and resulted in a 17% error when applied to a small sample of field observations. While the work with the SA model demonstrated the use of simulated data to train a neural network, the usefulness of the resulting algorithms would seem to be limited by the simplicity of the SA model that requires input at only two wavelengths, 440 and 550 nm. Such a model will never lead to "hyperspectral" algorithms since the entire remote sensing reflectance spectrum is determined from only two wavelengths. We follow the approach of Lee *et al.*, (1998a), but replace their two-wavelength model with the full spectral capability of the HYDROLIGHT radiative transfer model (Mobley, 1994 and 1998). We do not obtain spectral absorption and scattering by interpolation/extrapolation from data at 440 and 550 nm, but require hyperspectral measurements of absorption, and scattering as HYDROLIGHT inputs. HYDROLIGHT runs much more slowly than a simple SA model and is dependent on hyperspectral field data. However, these disadvantages are necessary to obtain true hyperspectral algorithms for hyperspectral sensors.

SIMULATED TRAINING SET

Hyperspectral absorption and beam attenuation data collected by Alan Weidemann of the Naval Research Laboratory in the coastal waters of the West Florida Shelf provided water optical properties for a series of HYDROLIGHT runs. These field data were collected at approximately 50 stations ranging from very turbid waters within Tampa Bay to clear offshore waters. The HiSTAR instrument that collected these field data experienced calibration problems. We attempted to correct these by using the more reliable AC9 instrument to perform a vicarious calibration of HiSTAR. For this paper we focus on bathymetry retrieval over sandy bottoms, therefore four sand bottom types were included in the HYDROLIGHT runs. These bottom types included coral sand (Maritorina, *et al.*, 1994), a sand from the Bahamas measured during the ONR CoBOP field program (Charles Mazel, personal communication), and two sands measured locally: in the Mississippi Sound and on Ship Island. There were 1124 HYDROLIGHT runs made with these four sand bottoms. The coral, Bahamas, Mississippi Sound, and Ship Island bottoms appeared in 544, 201, 107, and 272 HYDROLIGHT runs, respectively. Figure 1 shows the reflectance spectra of these sandy bottoms. The spectral shapes are similar except for the Bahamas sand which has a dip at 670 nm, possibly indicating a Chlorophyll-bearing organic component to the sediment. The Mississippi Sound sand has just a hint of the 670 nm dip also. The overall reflectance levels vary considerably with coral and Bahamas cases having the highest reflectance, Mississippi Sound the lowest, and Ship Island falling between. HYDROLIGHT runs included depths from 0 to 20 meters, wind speed from 0 to 10 m/s, and solar zenith angles from 0 to 50 degrees. We used the Petzold "average particle" phase function to describe particulate scattering (Petzold, 1972). HYDROLIGHT was set up to produce radiance and remote

sensing reflectance data at 5 nm intervals over the 400 to 750 nm spectral range (70 wavelengths). To use this data for algorithms for specific sensors, such as the HyMap system used here, the HYDROLIGHT output spectra were resampled by interpolation to match the center point of the spectral bands of the sensor of interest. No attempt has been made to account for HyMap bandwidth and spectral response function. The seventy HYDROLIGHT wavelengths were resampled to 21 bands corresponding to HyMap channels falling in the 400 to 750 nm range. The neural network training and test sets consisted of 1124, 22 component vectors where the first 21 components are spectral remote sensing reflectance values and the last component is depth of the water.

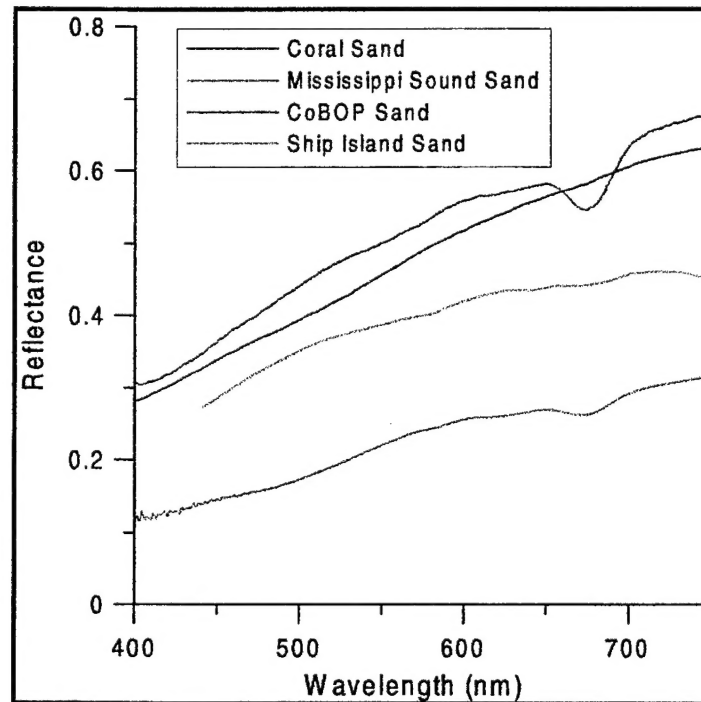


Figure 1 Bottom reflectance curves used to generate simulated data.

NEURAL NETWORKS

A neural network is a parallel computing architecture that can be trained by supervised learning to perform nonlinear mappings from one vector space to another. [See Lippman (1987) for an introduction to neural networks, or Haykin (1994) for a more complete treatment.] In the present case we solve a special case of the ocean optics inverse problem by mapping from a 21-dimensional remote sensing reflectance vector space into a one-dimensional vector space representing water depth. The processing conducted by each processing element (or neuron) in the network consists of forming a weighted sum of the inputs followed by a nonlinear transfer function to produce an output. The outputs thus produced by one layer of processing elements become the inputs to the next layer in the network. The "intelligence" in the network is contained in the weights that go into forming the sum in each processing element. The proper weight values are established by supervised learning using a training set of input vectors where

the corresponding output vector is known. The neural network used in this study is a feed-forward, fully connected net with an input layer (21 neurons), a hidden layer (10 neurons), and an output layer consisting of a single neuron.

Supervised training is accomplished by back propagation, which iteratively presents the spectral data as input and depth values as the corresponding desired output. Back propagation uses a gradient descent search technique to adjust network weights at each iteration to minimize the mean squared error between the desired output (known depth) and the actual network output. The training results in a network that produces least-squares estimates of depth given the spectrum of remote sensing reflectance. The network accuracy in general is tested utilizing an independent set of data not included in the training process.

NETWORK TRAINING

Training a neural network on modeled data presents some unusual problems. One problem is that the data is noise free. With noise-free data every digit is significant down to the limit of the floating-point precision of the computer running the radiative transfer model. If synthetic training data contains useful information at very low signal levels, such as remote sensing reflectance at 750 nm, the neural network will apply very large weights to these small but yet significant inputs in order to extract that information. This situation will produce good training statistics, but the resulting algorithm will not generalize well to real data. For example, if some residual reflected skylight is present in the 750 nm image, the reflectance value will not be small as in the training set, and the large weights applied to larger than expected input values will lead to erroneous depth retrievals. Other problems discussed later can also arise from "perfect" training data. To minimize these problems, the noise characteristics of the HyMap sensor were measured in an offshore portion of the HyMap image where the water is assumed to be uniform so that any variance in remote sensing reflectance within a box of pixels can be attributed to sensor noise. Normally distributed random noise with variance in each spectral band equal to that observed in HyMap imagery was added to the training set data produced by the HYDROLIGHT model. Addition of instrument noise to the training data is straightforward. However, how does one modify the training data to compensate for errors in sensor calibration, or more importantly errors in atmospheric correction of the airborne imagery? If the objective is to use modeled data for algorithms that will be applied to remotely sensed data these issues are significant.

Noise corrupted data from the 1124 HYDROLIGHT runs was split into training (1011 samples) and test (113 samples) sets. The neural network was trained to an rms error of 0.8 m between actual and estimated depths. The scatterplot for the training set is shown in Figure 2. Note that the error increases slightly with depth. One would expect to do better with optical retrieval of water depth in shallow water where the bottom reflected energy reaching the sea surface is larger. However, very accurate mappings of reflectance to depth were apparently obtained down to a depth of approximately 10 m. The rms error on the training set can also be expressed as a percentage of the depth value in which case the error is 9.4% which is about half of the 18% scatter reported by Lee *et*

al., (1998a). The rms error for the independent test set was 0.85 m (Figure 3). The neural network training has clearly resulted in a very good mapping of remote sensing reflectance spectra to water depth.

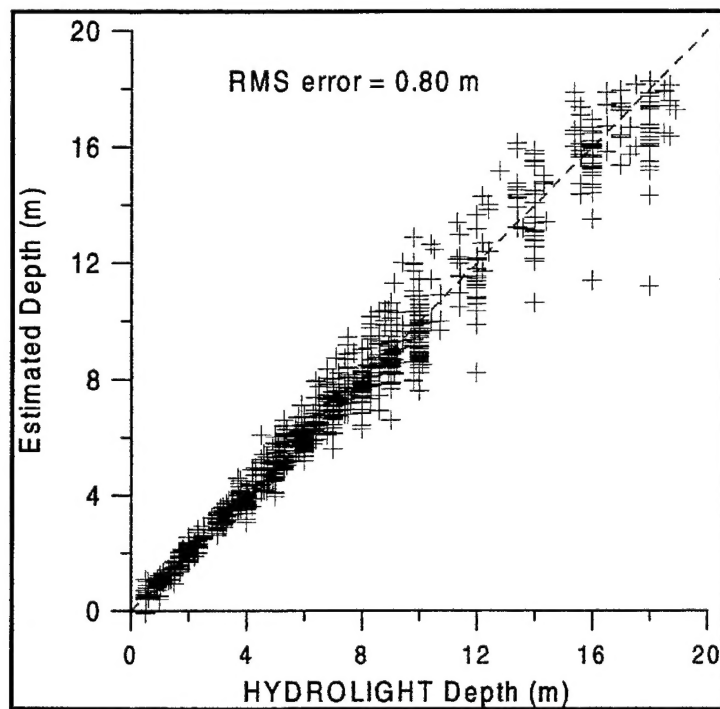


Figure 2 Scatterplot for neural network training set.

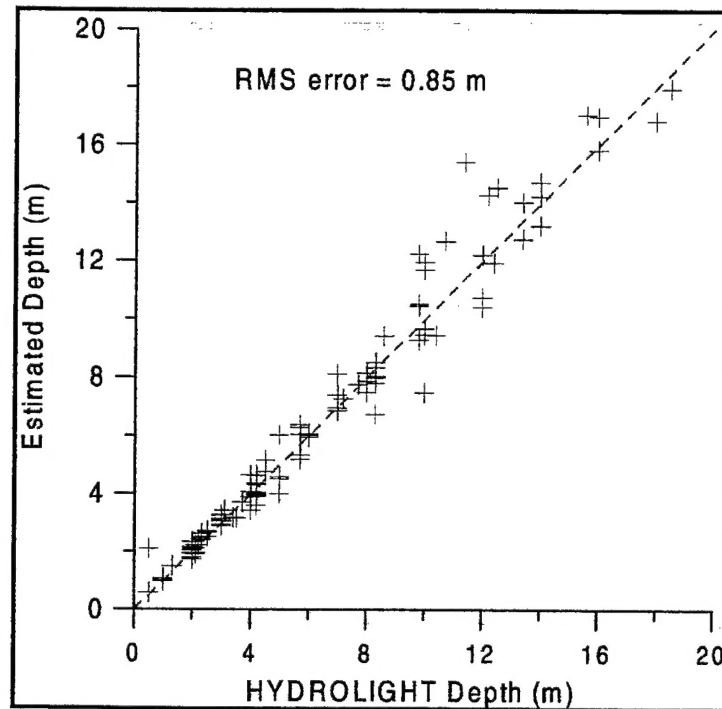


Figure 3 Scatterplot for neural network test set.

HYMAP IMAGERY

The HyMap sensor was flown over Ship Island off the coast of Mississippi on September 24, 1999. HyMap is a 126 channel instrument covering the spectral range 450 to 2500 nm. Signal-to-noise ratios are 500:1 or better in all channels. Analytical Imaging and Geophysics, LLC has calibrated, atmospherically corrected using ATREM (Goetz, *et al.* 1997)), geolocated the imagery, and has converted water-leaving radiance to remote sensing reflectance. Figure 4 is a color rendition of West Ship Island and surrounding shallows made from the HyMap imagery. Ground sampling distance for this imagery is 5 m. The first twenty-one HyMap channels fall within the 400 to 750 nm range of our simulated data set. The 21 spectral remote sensing reflectance values associated with each HyMap pixel can be processed by the trained neural network to produce a depth estimate for that location in the image.

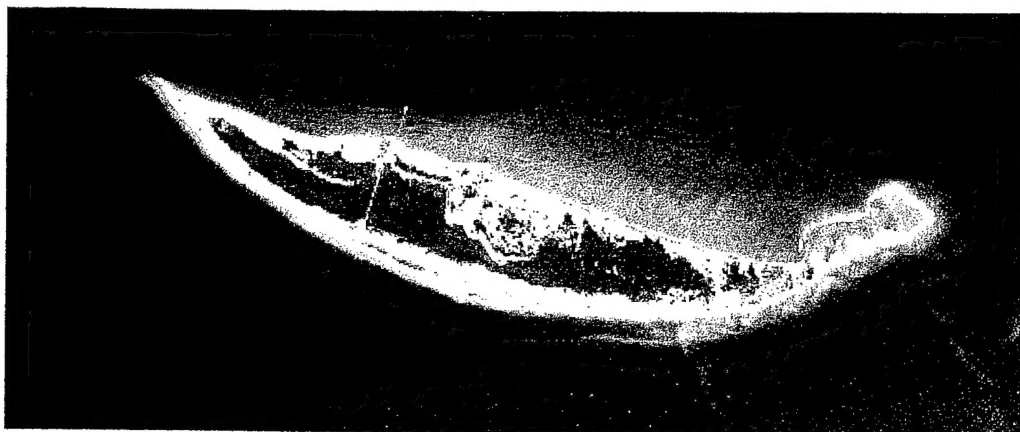


Figure 4 HyMap image of West Ship Island, MS.

RESULTS

We have a high quality, calibrated, atmospherically corrected hyperspectral image (Figure 4) that has been converted to remote sensing reflectance, and we have a neural network that accurately maps remote sensing reflectance spectra to water depth. It would seem straightforward to use the neural network to retrieve a reasonable water depth for each pixel location in the image. However, this straightforward step did not produce reasonable results. The direct application of the 21 input neural network to the image actually resulted in greatest depths near shore and shallower water offshore. This is a classic example of the difficulty of merging synthetic and real data. We believe that the neural network is "beating" one wavelength against another with very large weights of opposite signs. This situation works well on the clean, well-behaved simulated data as evidenced by the small scatter in Figures 2 and 3. However, these large weights applied to real data, which will have some differences from the simulated data, produces extraneous depth retrievals.

To avoid this problem, we reduced the number of neural network inputs to four. The inputs are remote sensing reflectance at 450, 550, and 650 nm and bottom reflectance at 550 nm (one of the parameters used in the SA model of Lee *et al.*, (1998a)). The reduced number of bands, plus some knowledge of bottom reflectance, eliminated the "beating" problem previously described. The training in this case resulted in an rms of 0.84 m for the training set and 0.83 m for the test set which is about the same as in the 21 input case. However, when we apply the smaller neural network to the HyMap data, the result is much better. The depth estimates for each pixel produced by the smaller network can be arranged in image format and depth encoded as a gray level to form a "depth image". Figure 5 is the depth image for West Ship Island produced by the small neural network. In Figure 5, lighter shades of gray represent shallower water and the shallower water is near the shore as expected. The depth range in Figure 5 is approximately 6 m, but there appears to be a bias of 1 m, *i.e.*, depth at the shoreline is 1 m above sea level.

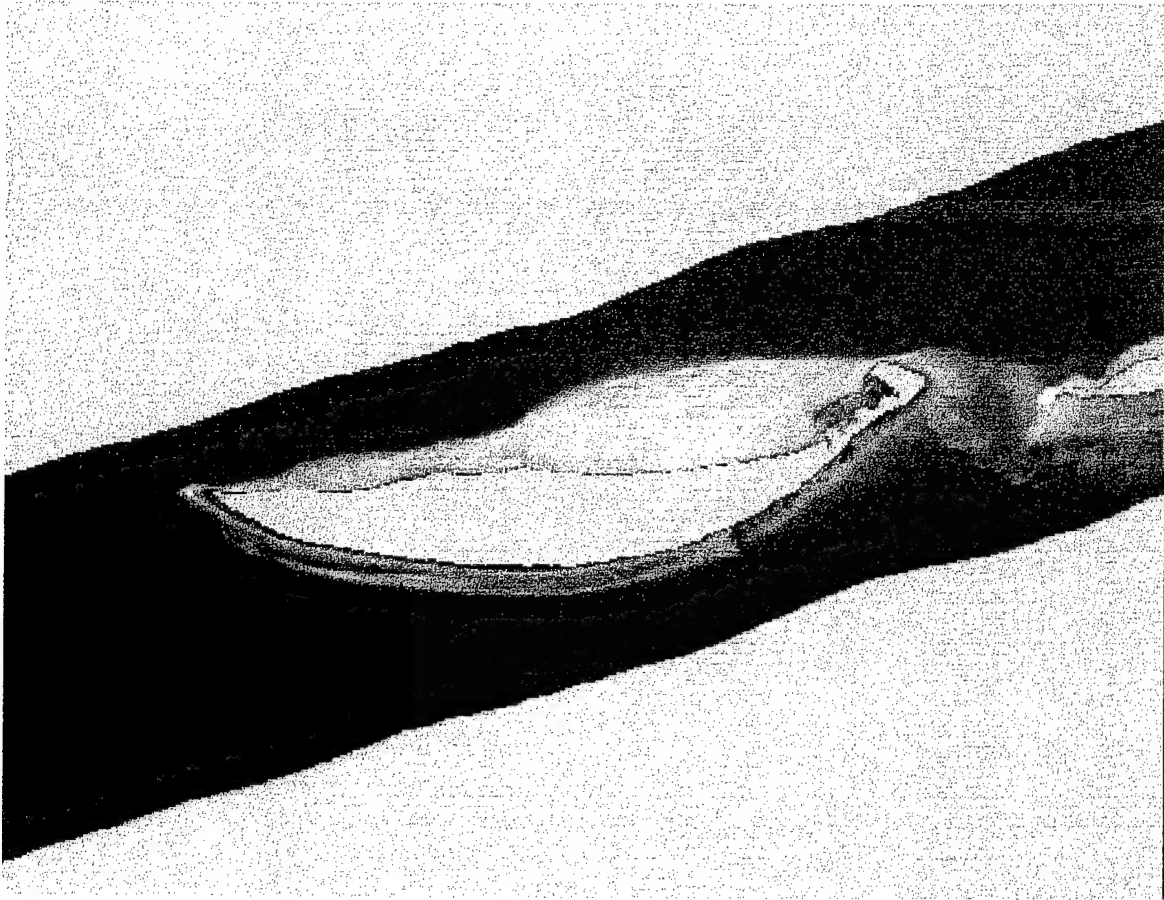


Figure 5 Depth image produced by application of a neural network to HyMap imagery.

DISCUSSION

Research quality depth data for the Ship Island area is not currently available for validation of the algorithm reported here. Bathymetric data collections in the near future will provide ground truth for this purpose. The best we can do presently is to present the NOAA chart for this area and make some preliminary comparisons. Figure 6 is a section of NOAA chart 11373_1.

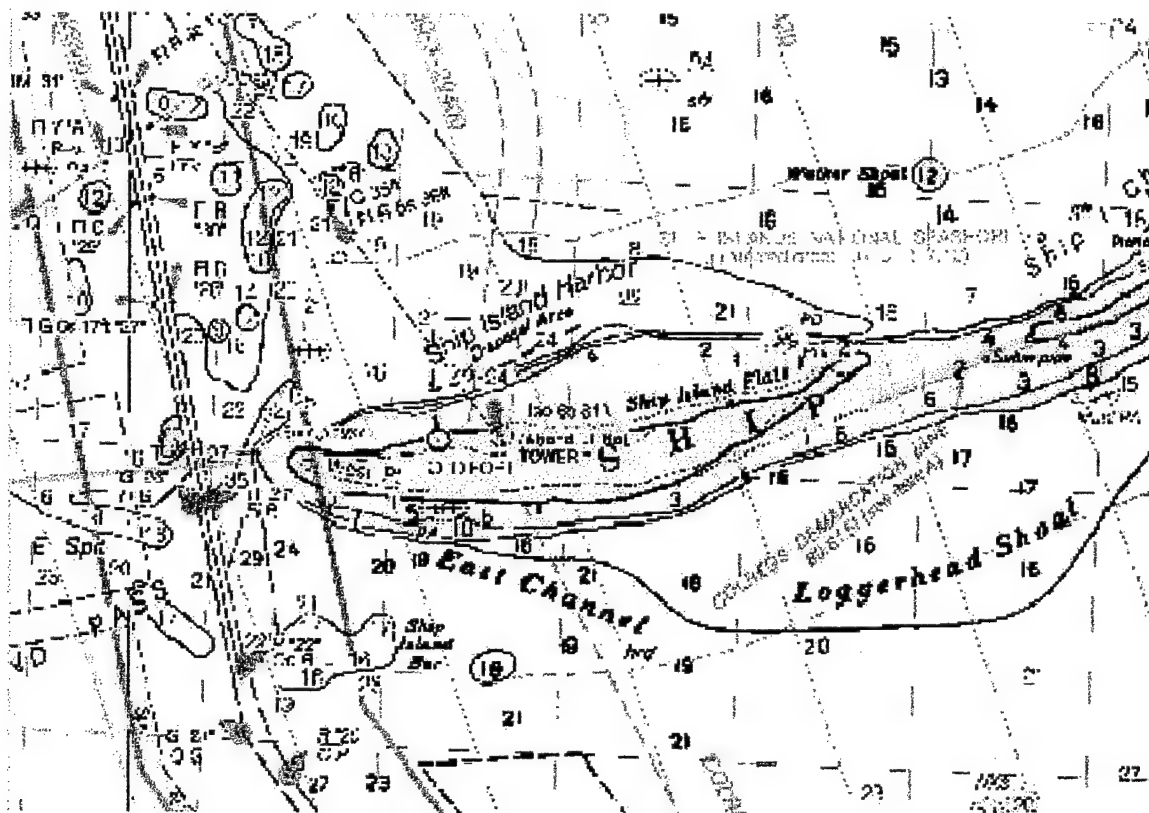


Figure 6 Section from NOAA Chart 11373_1.

Depths on the chart range over about 20 ft or 6 m, which agrees with the depth range in Figure 5. Note that the chart shows depths of 2 to 4 ft (~1 m) over the shoal on the north side of the island. Figure 5 from the HyMap image shows depths on the order of 1 m at this location also if the bias is removed. There is, therefore, general agreement between the chart and the hyperspectral depth retrievals. However, significant problems still remain and further work must be done to satisfactorily apply model-based algorithms to real data.

It would be interesting to compare the neural network approach reported here with the SA model of Lee *et al.*, (1998a,b). The SA model has been used to solve the radiative transfer inverse problem by iterative application of the forward model in an optimization scheme and has been applied to AVIRIS imagery in this fashion (Lee *et al.*, 1999 and 2000). In that work, as here, high quality ground truth data was not available for validation. Their conclusion when comparing the AVIRIS depth retrievals and NOAA charted depths was "that they both were quite consistent". A quantitative comparison should be made of the HYDROLIGHT/neural network and SA/optimization approaches.

The "beating" of one channel against another that is hypothesized to cause the poor retrievals here for the full 21 channel case is believed to occur because of the high degree of correlation between adjacent spectral bands. Another way of stating this is that

we have cast a low-dimensional problem into a high-dimensional spectral space and that dimensions in the high-order space, therefore, carry redundant information. The neural network training algorithm does undesirable things with this redundancy (lower accuracy). A logical solution to this problem would be to perform a principal components transformation on the spectral data. Principal components would result in new "bands" that are linear combinations of the original spectral bands, but that have the mathematical property of being uncorrelated (Ready and Wintz, 1973). These uncorrelated inputs to the neural network will eliminate the "beating" phenomenon. This hypothesis will be investigated and the results reported at the conference.

REFERENCES

- Goetz, A.F.H., J.W. Boardman, B. Kindel and K.B. Heidebrecht, "Atmospheric corrections: On deriving surface reflectance from hyperspectral imagers," *Proceedings SPIE Annual Meeting*, 3118, 14-22, 1997.
- Haykin, S. *Neural Networks: A Comprehensive Foundation*, Prentice Hall, 1994.
- Lippman, R.P., "An introduction to computing with neural nets," *IEEE ASSP Mag.* 4:4-22, 1987.
- Lee, Z.P., M.R. Zhang, K.L. Carder, and L.O. Hall, "A Neural Network Approach to Deriving Optical Properties and Depths of Shallow Waters," *Ocean Optics XIV*, Hawaii, October, 1998.
- Lee, Z.P., K.L. Carder, C.D. Mobley, R.G. Steward, and J.S. Patch, "Hyperspectral remote sensing for shallow waters: 1. A Semianalytical Model," *Appl. Opt.* 37, 6329-6338, 1998.
- Lee, Z.P., K.L. Carder, C.D. Mobley, R.G. Steward, and J.S. Patch, "Hyperspectral remote sensing for shallow waters: 2. Deriving bottom depths and water properties by optimization," *Appl. Opt.*, 38, 3831-3843, 1999.
- Lee, Z.P., K.L. Carder, and F.R. Chen, "Bathymetry and Environmental Properties Observed from AVIRIS Data," *Proc. Sixth Int. Conf. on Remote Sensing for Marine and Coastal Environments*, Charleston SC, Vol II, 143-148, 2000.
- Maritorena, Morel, and Gentili, "Diffuse Reflectance of Oceanic Shallow Waters: Influence of the Water Depth and Bottom Albedo," *Limnol. Oceanogr.* 39(7), 1689-1703, 1994.
- Mobley, C.D., *"Light and Water: Radiative Transfer in Natural Waters,"* Academic Press, 1994.
- Mobley, C.D., *"HYDROLIGHT 4.0 User's Guide,"* Sequoia Scientific, 1998.

Petzold, T.J., "Volume Scattering Functions for Selected Ocean Waters," SIO Ref. 72-78, Scripps Inst. Oceanogr., La Jolla, 1972.

Ready P.J. and P.A. Wintz, "Information Extraction, SNR Improvement and Data Compression in Multispectral Imagery," *IEEE Trans. On Communications*, **COM-21**(10), 1123-1131, 1973.

Sandidge, J.C. and R.J. Holyer, "Coastal Bathymetry from Hyperspectral Observations of Water Radiance," *Remote Sens. Environ.*, 65:431-352., 1998.

REMOTE SENSING ALGORITHMS BY NUMERICAL INVERSION OF RADIATIVE TRANSFER MODELS: NEURAL NETWORK AND OPTIMIZATION METHODS COMPARED

D.C. Hughes¹, R.J. Holyer¹, and Z.P. Lee²

¹ University of Southern Mississippi, School of Mathematical Sciences, Bldg. 9313, Rm 113, Stennis Space Center, MS, USA, 39529

² University of South Florida, Department of Marine Science
140 7th Ave. S., St. Petersburg, FL 33701

INTRODUCTION AND APPROACH

In ocean optics the forward problem (*i.e.*, given water optical properties and illumination conditions, find the water-leaving radiance) is solved and several computer implementations of in-water radiative transfer are available. Using these radiative transfer models, water-leaving radiance can be calculated with precision limited only by the availability of computer resources. However, the inverse problem (*i.e.*, given observations of water-leaving radiance, find the water and illumination conditions that necessarily lead to this observation) is not solved in closed analytical form. The inverse relationship may even be many-to-one. Moreover solution of the inverse problem is the essence of remote sensing, where the objective is retrieval of water depth, water inherent optical properties (IOPs), bottom reflectance (r_b), or some other parameter from observations of water-leaving spectral radiance or reflectance. In lieu of rigorous inversion, various empirical, semi-analytical, statistical, or numerical methods have been utilized for retrieval of ocean parameters from remotely sensed spectral radiance data. Two methods in particular have received recent attention. The methods are similar in many ways but quite different in implementation. Both methods have resulted in reasonable inversions of hyperspectral data. However, the two methods have never been applied to the same data set to allow quantitative comparisons. This paper presents the first comparison of this type. The methods are compared on the basis of accuracy, efficiency, robustness, and extension to complex coastal environments.

Both methods are based on radiative transfer models. Because the algorithms embody physics rather than statistical relationships, one would expect that both algorithms would be robust or universal in the sense that they would be applicable to many diverse water and bottom types. The first method (Lee *et al.*, (1999, 2001) solves the inverse problem by iteration in the forward direction. To provide an efficient forward calculation, a simplified forward radiative transfer model, the semi-analytical (SA) model, has been developed. The second algorithm uses a neural network (NN) trained using a large data set generated by HYDROLIGHT, a full forward radiative transfer model (Mobley, 1994), to produce a numerical inversion which takes the observed spectrum as input and generates a depth value or IOP value as output. Training of the NN is a global error minimization problem compared to the SA method which applies minimization for each pixel in the image. The SA approach embodies physics explicitly in the equations of the SA model. By contrast, the NN embodies physics implicitly by establishing numerical relationships between HYDROLIGHT calculated spectra and HYDROLIGHT input parameters such as water column absorption and scattering, r_b , and water depth. Since both methods use radiative transfer models, and

both use optimization/minimization, the essential difference focuses on philosophy of implementation.

NEURAL NETWORKS

A neural network is a parallel computing architecture that can be trained by supervised learning to perform nonlinear mappings from one vector space to another. [See Lippman (1987) for an introduction to neural networks, or Haykin (1994) for a more complete treatment.] In the present case we solve a subset of the ocean optics inverse problem by mapping from a multi-dimensional remote sensing reflectance (R_{rs}) vector space into a one-dimensional vector space representing water depth. The processing conducted by each processing element (or neuron) in the network consists of forming a weighted sum of the inputs followed by a nonlinear transfer function to produce an output. The outputs thus produced by one layer of processing elements become the inputs to the next layer in the network. The "intelligence" in the network is contained in the weights that go into forming the sum in each processing element. The proper weight values are established by supervised learning using a training set of input vectors where the corresponding output vector is known. The neural network used in this study is a feed-forward, fully connected net with an input layer, a hidden layer, and an output layer.

Supervised training is accomplished by back propagation, which iteratively presents the spectral data as input and depth values as the corresponding desired output. Back propagation uses a gradient descent search technique to adjust network weights at each iteration to minimize the mean squared error between the desired output (known depth) and the actual network output. The training results in a network that produces estimates of depth given the spectrum of R_{rs} . The network accuracy in general is tested utilizing an independent set of data not included in the training process. In this case the test set is taken from HyMaP imagery.

NEURAL NETWORK TRAINING SET

In Situ hyperspectral absorption and beam attenuation data in the coastal waters of the West Florida Shelf provided water optical properties for a series of HYDROLIGHT runs. These field data were collected at approximately 50 stations ranging from very turbid waters within Tampa Bay to clearer offshore waters. For this paper we focus on bathymetry retrieval over sandy bottoms, therefore, seven sand bottom types (coral sand, Biloxi sand, White bio-turbated sediment (CoBOP), CoBOP sand, Ship island sand, Ship Is. gulf, Ship Is. MS sound) were included in the HYDROLIGHT runs that included depths from 0 to 20 meters, wind speed from 0 to 10 m/s, and solar zenith angles from 10 to 50 degrees. HYDROLIGHT produced R_{rs} data at 5 nm intervals from 402.5 to 747.5 nm (70 wavelengths). To use this data for algorithms for specific sensors, such as the HyMaP system used here, the HYDROLIGHT output spectra were resampled by interpolation to match the center point of the spectral bands of the sensor of interest. No attempt has been made to account for HyMaP bandwidth and spectral response function. The seventy HYDROLIGHT wavelengths were resampled to 21 bands corresponding to HyMaP channels falling in the 400 to 750 nm range. The neural network training set consisted of 2118 samples. Random noise characteristic of the HyMaP sensor was added to the modeled data. The training vectors were also submitted to Principal Components Analysis (PCA) [See Davis (1986) for

an introduction| which reduced the number of bands in the imagery to four while conserving 99.85% of the total variance of the data set.

SEMI-ANALYTICAL MODEL

The semi-analytical model for shallow-water remote sensing simultaneously derives the bottom depth and water-column properties using an optimization approach. This approach takes a series of algebraic equations describing the absorption and scattering effects on the remote-sensing reflectance from the water column and optimizes using a predictor-corrector routine to minimize an error function. Each run in the forward direction produces a modeled spectrum that is matched with the observed spectrum. The error function calculates the root mean square between the observed R_{rs} and the modeled R_{rs} in the ranges 400-675nm and 750-830nm. For each set of R_{rs} values, the optimization program computes the error based on the five unknowns: absorption coefficient of phytoplankton pigment at 440nm, absorption coefficient of gelbstoff and detritus at 440nm, bottom reflectance at 550nm, water column depth, and a scattering factor which combines the particle-backscattering coefficient, viewing-angle information, as well as sea state. If the error statistic is larger than some acceptable tolerance level, the model parameters are adjusted according to the optimization scheme and the forward model is run again.

HyMaP IMAGERY

We apply both methods to two HyMaP hyperspectral images of Ship Is., MS. The HyMaP sensor was flown on 24 September 1999 and 11 May 2000. HyMaP is a 126-channel instrument covering the spectral range 450 to 2500 nm. Signal-to-noise ratios are

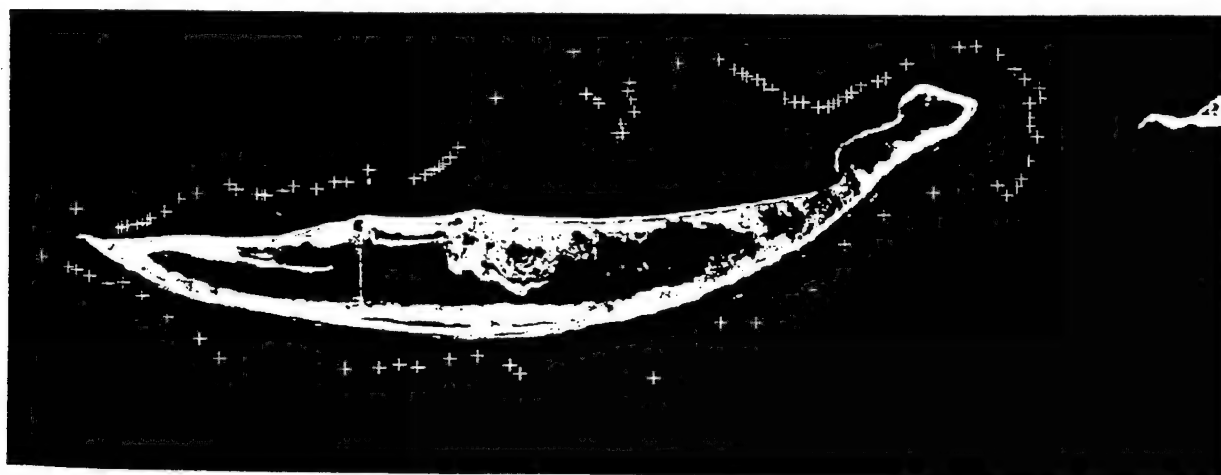


Figure 1 HyMaP image of West Ship Island, MS, 24 Sept. 1999.

500:1 or better in all channels. Analytical Imaging and Geophysics, LLC has calibrated, atmospherically corrected using ATREM (Goetz, *et al.* 1997)), geolocated the imagery, and has converted water-leaving radiance to R_{rs} . Figure 1 is a color rendition of West Ship Island and surrounding shallows made from the HyMaP imagery (24 September 1999). Ground sampling distance for this imagery is 5 m. We used only the first twenty-one HyMaP channels that fall within the 400 to 750 nm range. The ATREM process is intended for land imagery and does not include a correction for skylight reflected from the sea surface. HYDROLIGHT calculates a sky reflectance term which we subtracted from all HyMaP spectra. The white "+" symbols on the image mark the locations of known depths which will serve as ground truth for comparing the methods.

RESULTS

The trained NN with four principal components of noise-corrupted- R_{rs} as input was applied to the HyMaP test set to yield an overall rms error of 1.88 m. In the Ship Is. water we see evidence that bottom reflected light is insignificant in water deeper than 5 m. A more realistic statistic in this case would be to consider rms error in depth retrievals only for those samples in the 0 to 5 m range. In this case the rms error is reduced to 0.88 m.

As a benchmark for evaluating accuracy, we have calculated the rms error of a depth retrieval based on the mid-point of the range. That is, rather than use the NN or SA methods we will estimate the depth to be 2.5 m for all samples. In this case, which we will call the "no skill" method the rms error is 1.10 m. Our NN beats the no skill case.

The SA model is applied to the same test case of HyMaP spectra. It has been shown that the result of an optimization scheme is sensitive to the initial guess. The initial guess for

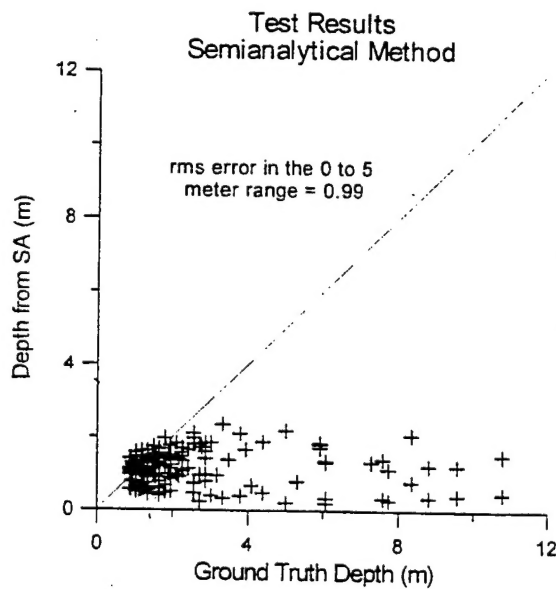


Figure 2

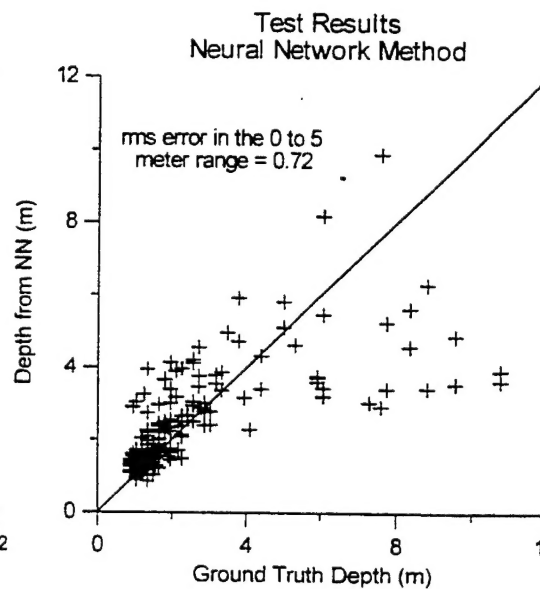


Figure 3

the iteration on each spectrum was chosen by picking characteristic samples from the test set from the image and adjusting the initial guess with respect to these parameters. Once a suitable initial guess was found, it was applied to all test set spectra. The rms error for the SA method is 2.54 m for the entire test set and 0.99 m for depths less than 5 m. Again, as with the neural network the SA method is better than the no skill method but not as good as the NN.

One way to improve the results of both methods is to supply knowledge about bottom reflectance. This can be done easily in this case since the beach is seen in the image. We have taken a pixel near the water (where the sand is believed to be wet) and found the reflectance value at 550 nm to be 0.2. This knowledge is input into the NN by training the NN with a fifth input (bottom reflectance) and then fixing this input at 0.2 when processing

the test set. The same information is supplied to the SA method by removing bottom reflectance as a free parameter of the optimization and fixing its value as 0.2 in the model. With bottom reflectance information added, the rms error of the NN method is reduced to 0.72 m and the rms error of the SA method increases to 4.65 m. Figures 2 and 4 show the

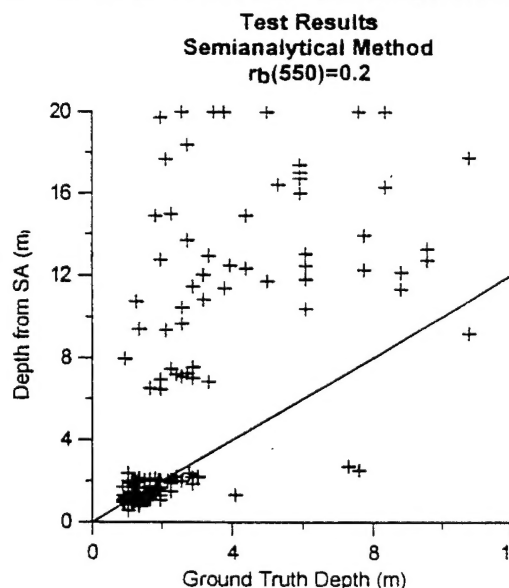


Figure 4

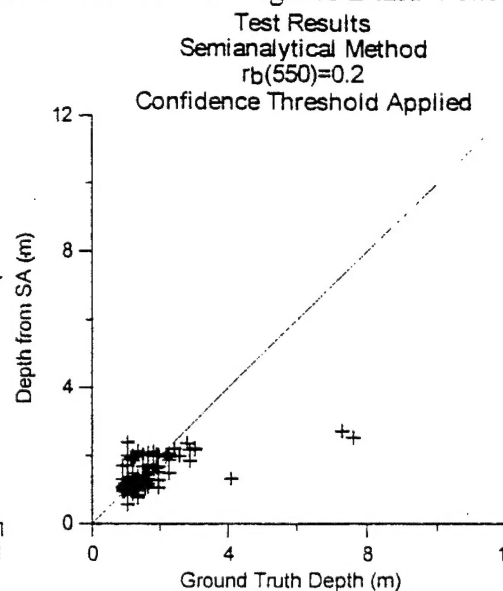


Figure 5

scatter plots of the SA model test set error without and with a fixed bottom reflectance, respectively. Figure 3 shows the scatter plot of the test set error for the NN. With regards to the results of Figure 4, we may attempt to improve the SA performance by introducing a "confidence parameter" to disregard those SA depths that do not have a significant contribution from the ocean bottom or that have some internal inconsistency in the solution. The use of such a parameter may limit the occurrence of outliers noticed in Figure 4; however, it also eliminates many samples where significant bottom reflectance actually occurred. Figure 5 shows the results of excluding low confidence depth retrievals (30% of all test samples excluded including 21% of samples of 0-5m depth).

SUMMARY AND DISCUSSION

The table below provides a summary comparison of the NN and SA methods.

FACTOR	NEURAL NETWORK	SEMI-ANALYTICAL
RTE Model	HYDROLIGHT	Up to 6 parameters (depth, bottom reflectance, absorption of gelbstoff, absorption of chlorophyll, a scattering term, and a spectral bias term)
Data Requirements for Algorithm Development	1) Hyperspectral <i>in situ</i> observations of IOPs and bottom reflectance 2) Large number (several thousand) of HYDROLIGHT files for a training set	None.
Potential Optical Complexity	Unlimited, can include fluorescence, Raman scattering, various scattering phase functions, etc.	Restricted by simplified model and by optimization speed and stability when number of parameters is large.
Ancillary Data Required for Algorithm Application	None.	Few estimates of depth, IOPs, and/or bottom reflectance are helpful for an optimization first guess. Solution shows dependency on first guess.

Parameter Optimized	Error in parameter retrieved (depth in this case)	Error in R_{rs} spectrum
Internal confidence measure	No.	Yes.
Parameters Retrieved	The one parameter NN is trained to retrieve.	All model parameters retrieved simultaneously.
Preprocessing of Image Data	NN approach uses PCA to decorrelate and reduce number of spectral bands.	None.
Accuracy of Depth Retrieval On HyMaP Test Images	rms = 0.72 m (0-5m depth, r_b known)	rms = 4.65 m (0-5m depth, r_b known) rms = 0.42 m (0-3m depth, r_b known, confidence threshold applied)

Although each method has its strengths and weakness as summarized in the table, in terms of accuracy of depth retrieval, the NN method has done significantly better for this data set unless a confidence filter has been used to discard many SA retrievals. What would explain this result? Errors in instrument calibration or atmospheric correction would degrade SA performance. However, these factors would also degrade NN performance and would not explain the accuracy difference unless the SA was much more sensitive to these factors than a more forgiving NN. Also one might suspect that there are water constituents in the Mississippi Sound that are not included in the SA model. It is possible that a more complex SA model allowing for additional water constituents would do better, although as the number of parameters in the SA model increases, convergence time and stability are expected to become problems. An examination of the spectral distribution of error in the SA model might help identify any missing constituents in the SA model. We also may have made poor initial guesses in optimization leading to less than optimal retrievals; however, observed variations with initial guess may be addressed with the use of the confidence term. An AVIRIS data set, on which the SA method has performed well in the past, will also be included in future studies to rule out the possibility that some problem might exist with the HyMaP data that is causing problems for the SA method. These factors are the topic of on going research which will lead to a more complete understanding of the characteristics of these methods.

REFERENCES

- Davis, John C. *Statistics and Data Analysis in Geology*. Wiley & Sons, Inc., 1986.
- Goetz, A.F.H., J.W. Boardman, B. Kindel and K.B. Heidebrecht, "Atmospheric corrections: On deriving surface reflectance from hyperspectral imagers," *Proceedings SPIE Annual Meeting*, 3118, 14-22, 1997.
- Haykin, S. *Neural Networks: A Comprehensive Foundation*. Prentice Hall, 1994.
- Lippman, R.P., "An introduction to computing with neural nets," *IEEE ASSP Mag.* 4:4-22, 1987.
- Lee, Z.P., K.L. Carder, C.D. Mobley, R.G. Steward, and J.S. Patch, "Hyperspectral remote sensing for shallow waters: 2. Deriving bottom depths and water properties by optimization," *Appl. Opt.*, 38, 3831-3843, 1999.

Lee, Z.P., K.L. Carder, R.F. Chen, T.G. Peacock, "Properties of the water column and bottom derived from Airborne Visible Infrared Imaging Spectrometer (AVIRIS) data," *J. Geophys. Res.*, Vol. 106 , No. C6 , p. 11,639, 2001.

Mobley, C.D., "*Light and Water: Radiative Transfer in Natural Waters*," Academic Press, 1994.